ACS Macro Letters

pubs.acs.org/macroletters Letter

Mobile Grafts Allow Polymers to Escape Confinement

Shivraj B. Kotkar, Michael P. Howard, Arash Nikoubashman, Jacinta C. Conrad,* Jeremy C. Palmer,* and Ryan Poling-Skutvik*

Cite This: https://doi.org/10.1021/acsmacrolett.6c00205 Read Online

ACCESS | Metrics & More | Article Recommendations | Supporting Information

ABSTRACT: Polymers attached to spherical particles are widely used in applications such as nanocomposites, drug delivery, and interfacial modification. In these systems, curvature-induced variations in monomer density lead to spatially dependent polymer chain structure and dynamics. Existing theories describing these effects assume that the polymer chains are anchored by immobile graft sites, but many experimental systems feature mobile or rearrangeable attachment points. Here, we use molecular simulations to show that the grafting site mobility significantly alters the dynamics of spherical polymer brushes. While both mobile and immobile grafts exhibit signatures of dynamic confinement near the particle surface, graft mobility reduces the extent of this confinement and shifts the crossover to unconfined dynamics. We quantify these effects through changes in the confinement length scale and the radial position at which confined dynamics disappears. In mixed systems, mobile grafts further facilitate the relaxation of neighboring immobile chains, establishing graft mobility as an important factor governing polymer dynamics in spherical polymer brushes.

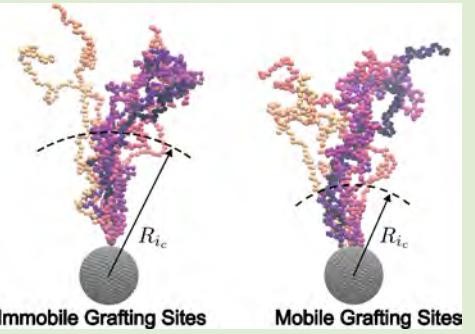

Polymer brushes are widely employed to control interfacial structure, interactions, and transport properties.[1−11] The covalent tethering of polymer chains to a surface significantly alters their conformations to be more stretched[12−16] and more slowly relaxing.[17,18] Additionally, the increased crowding of monomers near the surface can result in collective fluctuations involving many interacting chains.[19−24] For polymers grafted to spherical nanoparticles (NPs), surface curvature produces a radial dependence to monomer concentration and chain conformations,[25−28] resulting in a transition from a concentrated polymer brush regime near the surface to a semidilute brush regime toward the periphery.[29−32]

These distinct structural differences of grafted chains are also accompanied by pronounced changes in their dynamics. Relaxation times in dense brushes increase strongly with chain length and grafting density,[33,34] depend on monomer position along the chain and radial distance from the surface,[32,35] and often deviate from simple exponential decay.[32,36,37] Neutron spin-echo measurements further reveal signatures of confined dynamics and incomplete relaxation in dense brush regions near the NP surface.[36−38] The radial dependence of the polymer dynamics was confirmed using molecular dynamics[39] and dissipative particle dynamics simulations.[40] Our recent molecular simulation study of spherical polymer brushes elucidated the mechanism underlying these confined dynamics.[41] Specifically, we found that signatures of confined motion disappear at a radial distance that coincides with the crossover from the concentrated to the semidilute brush regimes, establishing a direct link between brush structure and local polymer relaxation dynamics.

To date, investigations of spherical polymer brush dynamics have largely focused on systems in which the grafting sites are immobile and remain in fixed positions on the NP surface. However, in many experimental systems, polymers may instead be tethered to fluid or deformable interfaces (e.g., lipid bilayers,[42] vesicles,[43] and emulsions[44−46]) as well as through reversible anchoring points (e.g., Au-Thiol chemistry[47,48]), allowing grafting sites to move laterally. Such graft mobility introduces an additional degree of freedom that can redistribute local crowding and modify relaxation pathways, altering polymer dynamics in spherical brushes. These changes may in turn influence nanocomposite rheology, nanoparticle self-assembly, the transport of small molecule penetrants in catalysis and separation applications, and the controlled release of theranostics. Nonetheless, understanding of the influence of grafting site mobility on polymer dynamics in spherical brushes remains poorly understood.

Here, we investigate the dynamics of polymers grafted to spherical NPs with mobile attachment points. Using molecular simulations that explicitly resolve both chain motion and graft rearrangement, we examine how graft mobility alters spatially heterogeneous relaxation dynamics relative to brushes with fixed grafting constraints. We find that graft mobility allows

Received: April 8, 2026
Revised: May 12, 2026
Accepted: May 13, 2026

polymer brushes to escape dynamical confinement more readily than comparable chains with immobile grafting sites. Remarkably, in both cases, this confinement scales with the grafting density according to the grafted polymer structure.

We performed molecular dynamics (MD) simulations with HOOMD-blue 2.9.2[49] to study effects of grafting mobility on the dynamics of chains end-grafted to a spherical NP. Model parameters and physical quantities are reported in implicit dimensionless form in which a, m, ε, and $\tilde{t} = \sqrt{ma^2/\varepsilon}$ are defined as the fundamental units for length, mass, energy, and time, respectively. The polymers were modeled as Kremer–Grest chains,[50] each containing 120 monomers with diameter $a_p = 1$ adjoined by finite extensible nonlinear elastic (FENE) bonds.[51] The NP was modeled as a sphere with radius $R_{NP} = 5$, consisting of 642 monomer-sized surface beads positioned at the vertices generated by recursively subdividing the faces of a regular icosahedron into equilateral triangles.[52,53] For brushes with immobile grafting sites (IGS), a FENE bond was used to adjoin one of the terminal monomers on each polymer chain to an NP surface bead. For brushes with mobile grafting sites (MGS), a harmonic potential was used to restrain one of the terminal monomers at roughly the same radial distance from the NP's center of mass ($\approx R_{NP}+a_p$) without imposing any restrictions on the angular position. To mimic good solvent conditions, a purely repulsive Weeks–Chandler–Andersen (WCA) potential[54] was used to model excluded volume interactions between monomer–monomer and monomer–NP beads. All simulations were performed at a reduced temperature $T = 1$.

We examined systems with reduced grafting densities $\gamma = \sigma R_{g,0}^2$ from 0.46 to 50, covering the same range as our previous computational and experimental studies,[37,41] where $R_{g,0} = 8.3$ is the root-mean-square radius of gyration of a free 120-mer chain in an infinitely dilute solution. Dynamics of the grafted chains were characterized by computing the time-dependent mean square angular displacement (MSAD) of individual monomers

$$\langle [\theta_i(t)]^2 \rangle = \left\langle \left[\arccos\left(\frac{\mathbf{r}_i(t)\cdot\mathbf{r}_i(0)}{|\mathbf{r}_i(t)||\mathbf{r}_i(0)|} \right) \right]^2 \right\rangle \quad (1)$$

where i is the monomer index (1 for the grafted monomer and 120 for the free end) and $\mathbf{r}_i$ is the position vector for monomer i relative to the center of the NP. The angle brackets $\langle \cdots \rangle$ denote that the average is taken over multiple time origins with the same lag time t for monomers with the same index on different chains. Additional details of the model, simulation protocols, and analysis procedures (including discussion of the MSAD versus using the standard mean square displacement (MSD)) are presented in Supporting Information.

To probe chain segmental dynamics as a function of the radial distance from the NP surface, we examine the MSAD as a function of monomer index i for various grafting densities (Figure 1). On short time scales, the dynamics of monomers on chains in brushes with IGS and MGS are nearly indistinguishable and exhibit subdiffusive scaling with $\langle [\theta_i\ (t)\ ]^2 \rangle \sim t^{\alpha}$, where $\alpha \approx 1/2$, approximately following Rouse predictions for segmental fluctuations. Increasing grafting density γ results in a concomitant decrease in the short-time MSAD, reflecting the slowing of the segmental motions as the local friction from interactions with neighboring chains is enhanced. On long time scales, the MSAD saturates

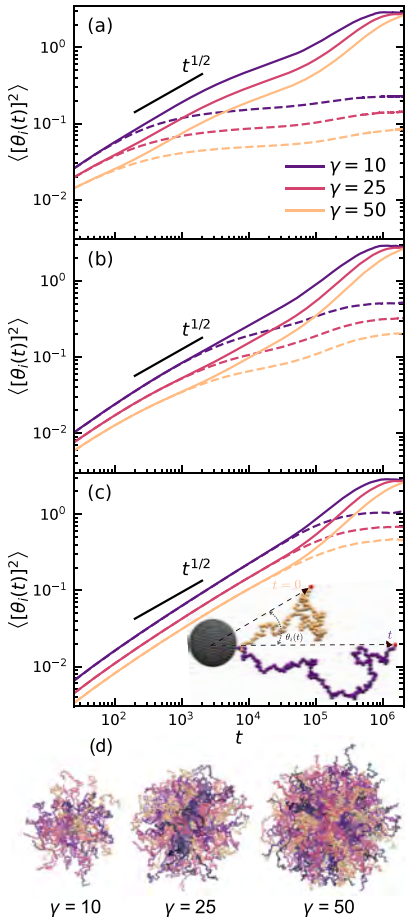

Figure 1. Mean square angular displacement $\langle [\theta_i(t)]^2 \rangle$ of monomer (a) $i = 10$, (b) $i = 30$, and (c) $i = 120$ at $\gamma = 10$, 25, and 50 for polymers with immobile grafting sites (IGS, solid lines) and mobile grafting sites (MGS, dashed lines). Inset to (c): schematic identifying the angular displacement $\theta_i(t)$ for a monomer i. (d) Renderings of spherical brush systems at three different grafting densities.

at a terminal plateau. For brushes with IGS, the MSAD saturation value increases with monomer index i, suggesting that monomers farther from the NP surface can sample larger angular fluctuations. For the same monomer index i, the saturation values decrease with an increase in grafting density γ, due to the increased steric hindrance from neighboring chains. For brushes with MGS, by contrast, the saturation value is independent of both monomer index and grafting density, but the time required to reach saturation increases with the latter. Hence, the chains are able to fully explore the NP surface given sufficient time, albeit more slowly as it becomes increasingly crowded with chains. The observed MSAD saturation behavior for brushes with IGS and MGS is consistent with theoretical predictions from corresponding analytical models (Supporting Information).

To characterize the confinement length associated with these intermediate plateaus, we fit $\log_{10}\langle [\theta_i(t)]^2 \rangle$ to cubic polynomials and use the inflection point to precisely quantify the plateau height (Supporting Information). The corresponding confinement length scale is calculated as $l_c = R_i \langle [\theta_i(t_c)]^2 \rangle^{1/2}$, where t_c is the time at which the inflection point occurs, and R_i is the average distance of the i-th monomer from the center of the NP. This definition converts the angular dynamics to linear spatial dimensions, with l_c being

https://doi.org/10.1021/acsmacrolett.6c00205
ACS Macro Lett. XXXX, XXX, XXX−XXX

the effective arc length sampled by the monomers at the intermediate time plateau in the MSAD. The confinement length increases with i as monomers are farther from the particle surface (Figure 2), as we previously found.[41]

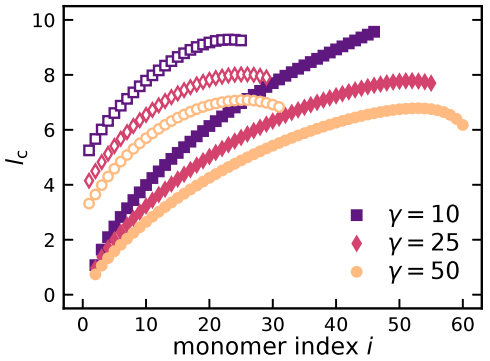

Figure 2. Confinement length l_c as a function of monomer index i for chains with IGS (closed symbols) and MGS (open symbols).

Intriguingly, chains with MGS have a larger l_c than those with IGS at comparable i. For chains with both IGS and MGS, l_c decreases with increasing γ as chains get closer together. Furthermore, there is a critical monomer index i_c at which the intermediate plateaus disappear and the monomer dynamics are no longer confined. This index is much higher for chains with IGS than for those with MGS, increasing from $i_c = 25$ for MGS to $i_c = 46$ for IGS at $\gamma = 10$. From these observations, we conclude that MGS reduces confinement in two ways. First, MGS allows monomers to sample larger lateral fluctuations before experiencing confinement from neighboring chains, resulting in the larger values of l_c. Second, steric interactions with neighboring chains persist over shorter radial distances for chains with MGS, enabling monomers closer to the particle surface to escape confinement and reducing the value of i_c.

Thus far, we have interpreted the confined dynamics observed for chains with both IGS and MGS to steric interactions between neighboring chains. To gain insight into the mechanisms underlying this confinement, we examine the average distance R_{i_c} of the critical monomer i_c from the NP center as a function of grafting density γ (Figure 3). Structurally, the extended Daoud−Cotton (EDC) theory[25,27] predicts that grafted chains transition from a concentrated polymer brush (CPB) regime to a semidilute polymer brush (SDPB) regime at a critical radius $R_{CPB} = R_{NP} b R_{g,0}^{-1} \tilde{\nu}^{-1} \gamma^{1/2}$, where b is the effective bond size that characterizes the cross-sectional area of the chain and $\tilde{\nu} = \nu/\sqrt{4\pi}$ is a rescaled excluded volume parameter. This critical radius R_{CPB} scales with $\gamma^{1/2}$ and quantifies the distance from the NP center at which steric interactions governing chain extension weaken sufficiently for the polymer chains to adopt a swollen coil conformation.[30] In previous work,[41] we found that R_{i_c} at which chain dynamics are no longer confined also scales with $\gamma^{1/2}$, indicating that this *dynamic* mode is controlled by a *structural* transition.

We conduct a similar analysis for chains with MGS and again find that $R_{i_c} \sim \gamma^{1/2}$ (Figure 3). This scaling confirms that grafted chains, regardless of the mobility of the grafting site, exhibit confined dynamics near the particle surface due to steric interactions with neighbors and escape confinement once those steric interactions become sufficiently weak, in an

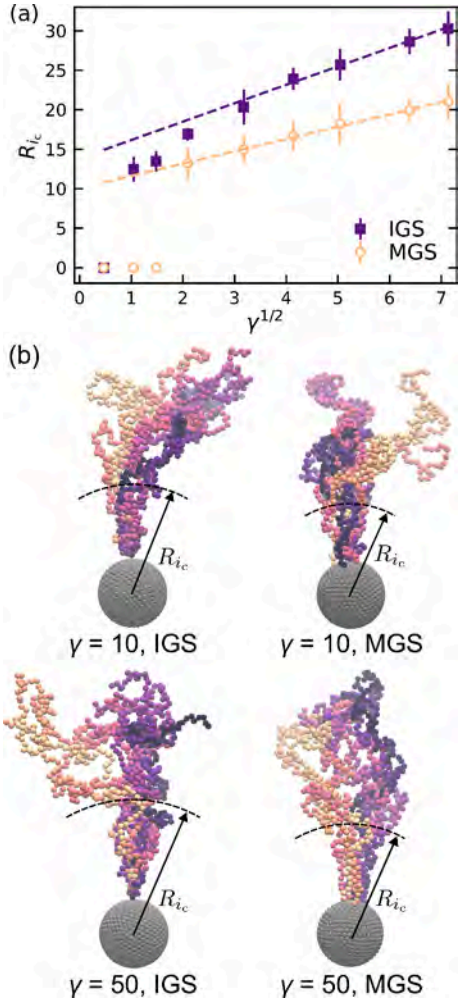

Figure 3. (a) Scaling of the critical radius R_{i_c} at which monomers no longer exhibit a confinement plateau as a function of the square root of grafting density $\gamma^{1/2}$ for chains with IGS and MGS. (b) Representative chain conformations over $n = 10$ time points for IGS and MGS chains at $\gamma = 10$ and $\gamma = 50$. Only one chain per particle shown for clarity.

analogous fashion to the structural transition between CPB and SDPB regimes. Despite similar scaling, R_{i_c} is significantly lower for chains with MGS relative to those with IGS, indicating that the grafting site mobility facilitates more rapid escape of monomers from confinement. Furthermore, R_{i_c} for MGS chains has a shallower slope with respect to $\gamma^{1/2}$. Mathematically, according to the structural interpretation of EDC theory, this slope depends on R_{NP}, $\tilde{\nu}$, and b, but R_{NP} does not vary between simulations with fixed and mobile sites and $\tilde{\nu}$ should not vary significantly for these systems because of the quantitatively identical monomer density profiles (Supporting Information). The decreased slope for MGS chains therefore suggests that the grafting site mobility affects the relationship between the cross-sectional area of the chain characterized by b and the dynamical transition from confined to unconfined relaxations.

Additionally, in the limit of $\gamma \to 0$, R_{i_c} is considerably smaller than expected from the predicted scaling for chains with IGS and MGS (Figure 3). This deviation is more dramatic for chains with MGS where monomers are no longer confined

https://doi.org/10.1021/acsmacrolett.6c00205
ACS Macro Lett. XXXX, XXX, XXX−XXX

even at finite grafting densities, whereas confinement disappears only in the limit $\gamma \to 0$ for chains with IGS. This observation is consistent with our posited physical mechanism in which MGS allow chains to move past one another to facilitate escape from a local confinement tube. This mechanism is in close analogy to the concepts of constraint release[55] or contour length fluctuations[56] for entangled polymer melts, wherein the mobility of neighboring chains leads to faster chain relaxations than expected for classical reptation.[57] Thus, although chains with MGS still exhibit confined dynamics due to steric interactions with neighboring chains, the mobility of the grafting site relaxes this confinement, allowing chains to fluctuate over longer distances and escape the confinement tube more readily.

As a final test of the impact of grafting site mobility on chain dynamics, we conduct simulations in which a fraction f of chains has MGS and the rest have IGS. An increase in f results in an increase in the MSADs for both IGS chains (Figure 4(a)) and MGS chains (Supporting Information) on intermediate and long time scales. Dynamics on shorter time scales are unaffected by f, because chain fluctuations are unconfined. We quantify the reduction in dynamical confinement through R_{i_c} using only the dynamics of the IGS chains rather than averaging across both IGS and MGS populations. Consistent with the qualitative observations from the MSADs, R_{i_c} decreases monotonically with f from the most confined case of all IGS chains to the least confined case of all MGS chains (Figure 4(b)). Thus, the presence of MGS chains helps to relax the confinement experienced by the IGSs.

We rationalize this collective impact through the scaling of the critical radius R_{i_c} with grafting density γ. For mixtures of MGS and IGS chains, we find that $R_{i_c} \sim \lambda(f) b \gamma^{1/2}$ (Figure 4(c)), where $\lambda(f)$ is a dynamical reduction factor that modifies how the effective cross-sectional area of a chain impacts the confined dynamics. Defining $\lambda = 1$ for fully IGS chains, the introduction of MGS chains causes a monotonic decrease in λ to a limiting value of $\lambda \approx 0.66$ for fully MGS chains. Physically, the reduction in λ demonstrates that MGS chains contribute less significantly to dynamical confinement and facilitates more rapid escape from confinement even for neighboring IGS chains. We note that this impact of MGS chains occurs without any discernible change in the grafted polymer *structure*, indicating that the relationship between structure and dynamics for grafted systems depends strongly on grafting site mobility.

In summary, our simulations investigate the effect of grafting site mobility on the confined dynamics of polymer chains attached to spherical particles. We find that MGS chains exhibit qualitatively similar confinement to IGS chains, characterized by a plateau in the MSADs on intermediate time scales, but that this confinement is quantitatively weaker for MGS chains. For MGS chains, the confinement length l_c is significantly larger and disappears at lower monomer indices, resulting in a decrease in the critical radius R_{i_c} that quantifies the transition from confined to unconfined dynamics. Furthermore, by simulating mixtures of IGS and MGS chains, we find that IGS chains can more readily escape confinement in the presence of MGS chains through a dynamical reduction in the effective cross-sectional area of the chains. We expect that this dynamical confinement depends not only on the parameters varied here (i.e., grafting site mobility and grafting density) but also on the nanoparticle radius, chain stiffness, and intermolecular interactions, all of which will be the focus of future simulations. Our findings extend the relationship between structure and dynamics of grafted polymers to polymers attached to fluid interfaces, such as lipid bilayers,[42] vesicles,[43] and emulsions.[44−46] We anticipate that these simulations will motivate experimental investigations of the confined dynamics of mobile grafting chains using dynamical techniques, such as neutron spin-echo spectroscopy, which could reveal faster relaxations or reduced plateaus in the intermediate scattering function[37] relative to polymers grafted to comparable solid particles.

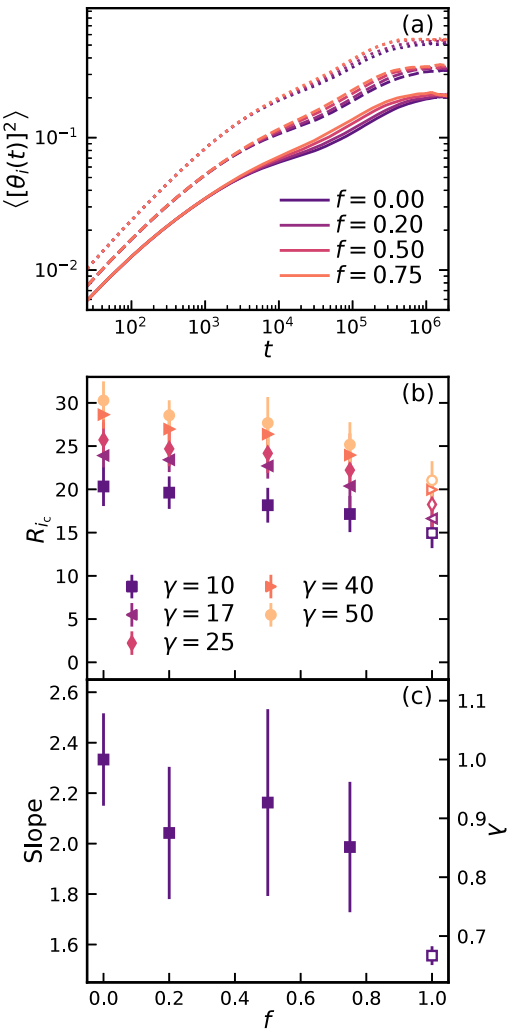

Figure 4. (a) Mean square angular displacement $\langle[\theta_i(t)]^2\rangle$ of monomer $i = 30$ on chains with IGS for $\gamma = 10$ (dotted lines), $\gamma = 25$ (dashed lines), and $\gamma = 50$ (solid lines) with varying fraction f of MGS chains. (b) Critical radius R_{i_c} for IGS chains (closed symbols) and MGS chains (open symbol) as a function of f. (c) The slope of R_{i_c} with $\gamma^{1/2}$ as a function of f for IGS chains (closed symbols) and for chains where all chains are MGS (open symbols). The corresponding value for the dynamic reduction factor λ is shown on the right.

■ ASSOCIATED CONTENT

Supporting Information

The Supporting Information is available free of charge at https://pubs.acs.org/doi/10.1021/acsmacrolett.6c00205.

https://doi.org/10.1021/acsmacrolett.6c00205
ACS Macro Lett. XXXX, XXX, XXX−XXX

Detailed computational methods, additional simulation data, and example analyses (PDF)

AUTHOR INFORMATION

Corresponding Authors

Jacinta C. Conrad − *Department of Chemical and Biomolecular Engineering, University of Houston, Houston, Texas 77204, United States;* orcid.org/0000-0001-6084-4772; Email: jcconrad@uh.edu

Jeremy C. Palmer − *Department of Chemical and Biomolecular Engineering, University of Houston, Houston, Texas 77204, United States;* orcid.org/0000-0003-0856-4743; Email: jcpalmer@uh.edu

Ryan Poling-Skutvik − *Department of Chemical, Biomolecular, and Materials Engineering, University of Rhode Island, Kingston, Rhode Island 02881, United States; Department of Physics, University of Rhode Island, Kingston, Rhode Island 02881, United States;* orcid.org/0000-0002-1614-1647; Email: ryanps@uri.edu

Authors

Shivraj B. Kotkar − *Department of Chemical and Biomolecular Engineering, University of Houston, Houston, Texas 77204, United States;* orcid.org/0000-0001-6051-9363

Michael P. Howard − *Department of Chemical Engineering, Auburn University, Auburn, Alabama 36849, United States;* orcid.org/0000-0002-9561-4165

Arash Nikoubashman − *Leibniz-Institut für Polymerforschung Dresden e.V., 01069 Dresden, Germany; Institut für Theoretische Physik, Technische Universität Dresden, 01069 Dresden, Germany;* orcid.org/0000-0003-0563-825X

Complete contact information is available at: https://pubs.acs.org/10.1021/acsmacrolett.6c00205

Notes

The authors declare no competing financial interest.

ACKNOWLEDGMENTS

This research was supported by the National Science Foundation (CBET-2339052 to R.P.-S., CBET-2223084 to M.P.H., and CBET-2529134 to J.C.C. and J.C.P.) and by the Deutsche Forschungsgemeinschaft (DFG, German Research Foundation) through the Heisenberg grant (Project No. 470113688 to A.N.). Acknowledgment is also made to the donors of the American Chemical Society Petroleum Research Fund (Grant No. 66616-DNI9 to M.P.H.) and to the Welch Foundation (E-1869 to J.C.C, E-1882 to J.C.P.) for support of this research. Computational resources were provided by the Hewlett-Packard Enterprise Data Science Institute at the University of Houston and the Texas Advanced Computing Center at the University of Texas at Austin.

REFERENCES

(1) Akcora, P.; Liu, H.; Kumar, S. K.; Moll, J.; Li, Y.; Benicewicz, B. C.; Schadler, L. S.; Acehan, D.; Panagiotopoulos, A. Z.; Pryamitsyn, V.; Ganesan, V.; Ilavsky, J.; Thiyagarajan, P.; Colby, R. H.; Douglas, J. F. Anisotropic self-assembly of spherical polymer-grafted nanoparticles. *Nat. Mater.* **2009**, *8*, 354−359.

(2) Chevigny, C.; Dalmas, F.; Di Cola, E.; Gigmes, D.; Bertin, D.; Boue, F.; Jestin, J. Polymer-Grafted-Nanoparticles Nanocomposites: Dispersion, Grafted Chain Conformation, and Rheological Behavior. *Macromolecules* **2011**, *44*, 122−133.

(3) Martin, T. B.; Mongcopa, K. I. S.; Ashkar, R.; Butler, P.; Krishnamoorti, R.; Jayaraman, A. Wetting-Dewetting and Dispersion-Aggregation Transitions Are Distinct for Polymer Grafted Nanoparticles in Chemically Dissimilar Polymer Matrix. *J. Am. Chem. Soc.* **2015**, *137*, 10624−10631.

(4) Kulshreshtha, A.; Jayaraman, A. Dispersion and Aggregation of Polymer Grafted Particles in Polymer Nanocomposites Driven by the Hardness and Size of the Grafted Layer Tuned by Attractive Graft-Matrix Interactions. *Macromolecules* **2020**, *53*, 1302−1313.

(5) Bilchak, C. R.; Jhalaria, M.; Huang, Y.; Abbas, Z.; Midya, J.; Benedetti, F. M.; Parisi, D.; Egger, W.; Dickmann, M.; Minelli, M.; Doghieri, F.; Nikoubashman, A.; Durning, C. J.; Vlassopoulos, D.; Jestin, J.; Smith, Z. P.; Benicewicz, B. C.; Rubinstein, M.; Leibler, L.; Kumar, S. K. Tuning selectivities in gas separation membranes based on polymer-grafted nanoparticles. *ACS Nano* **2020**, *14*, 17174−17183.

(6) Long, D.; Ajdari, A.; Leibler, L. How Do Grafted Polymer Layers Alter the Dynamics of Wetting? *Langmuir* **1996**, *12*, 1675−1680.

(7) Senaratne, W.; Andruzzi, L.; Ober, C. K. Self-Assembled Monolayers and Polymer Brushes in Biotechnology: Current Applications and Future Perspectives. *Biomacromolecules* **2005**, *6*, 2427−2448.

(8) Yadav, V.; Jaimes-Lizcano, Y. A.; Dewangan, N. K.; Park, N.; Li, T. H.; Robertson, M. L.; Conrad, J. C. Tuning Bacterial Attachment and Detachment via the Thickness and Dispersity of a pH-Responsive Polymer Brush. *ACS Appl. Mater. Interfaces* **2017**, *9*, 44900−44910.

(9) Li, T.-H.; Yadav, V.; Conrad, J. C.; Robertson, M. L. Effect of Dispersity on the Conformation of Spherical Polymer Brushes. *ACS Macro Lett.* **2021**, *10*, 518−524.

(10) Liu, X.; Yu, S.; Zhang, Y.; Zhang, Z.; Li, L.; Kelarakis, A.; Feng, B.; Li, J.; Ballauff, M.; Liao, Q.; Guo, X. Friction Control via Tunable Interpenetration of Spherical Polyelectrolyte Brushes. *Macromolecules* **2026**, *59*, 3487.

(11) Tian, X.; Chen, Y.; Xu, X.; Xu, W.-S.; Chen, J. Theory of mobility of inhomogeneous-polymer-grafted particles. *J. Chem. Phys.* **2023**, *158*, 204904.

(12) Alexander, S. Adsorption of chain molecules with a polar head: A scaling description. *J. Phys. (Paris)* **1977**, *38*, 983−987.

(13) de Gennes, P. G. Conformations of Polymers Attached to an Interface. *Macromolecules* **1980**, *13*, 1069−1075.

(14) Zhulina, E. B.; Borisov, O. V.; Priamitsyn, V. A. Theory of Steric Stabilization of Colloid Dispersions by Grafted Polymers. *J. Colloid Interface Sci.* **1990**, *137*, 495−511.

(15) Milner, S. T. Polymer Brushes. *Science* **1991**, *251*, 905−914.

(16) Karim, A.; Satija, S. K.; Douglas, J. F.; Ankner, J. F.; Fetters, L. J. Neutron Reflectivity Study of the Density Profile of a Model End-Grafted Polymer Brush: Influence of Solvent Quality. *Phys. Rev. Lett.* **1994**, *73*, 3407−3410.

(17) Aoki, H.; Kitamura, M.; Ito, S. Nanosecond Dynamics of Poly(Methyl Methacrylate) Brushes in Solvents Studied by Fluorescence Depolarization Method. *Macromolecules* **2008**, *41*, 285−287.

(18) Gianneli, M.; Roskamp, R. F.; Jonas, U.; Loppinet, B.; Fytas, G.; Knoll, W. Dynamics of Swollen Gel Layers Anchored to Solid Surfaces. *Soft Matter* **2008**, *4*, 1443−1447.

(19) de Gennes, P.-G. Dynamics of a Diffuse Layer of Adsorbed Polymer. *C. R. Acad. Sci. Paris Ser. II* **1986**, *302*, 765−768.

(20) de Gennes, P.-G. Polymers at an Interface; a Simplified View. *Adv. Colloid Interface Sci.* **1987**, *27*, 189−209.

(21) Farago, B.; Monkenbusch, M.; Richter, D.; Huang, J. S.; Fetters, L. J.; Gast, A. P. Collective Dynamics of Tethered Chains: Breathing Modes. *Phys. Rev. Lett.* **1993**, *71*, 1015−1018.

(22) Yakubov, G. E.; Loppinet, B.; Zhang, H.; Rühe, J.; Sigel, R.; Fytas, G. Collective Dynamics of an End-Grafted Polymer Brush in Solvents of Varying Quality. *Phys. Rev. Lett.* **2004**, *92*, 115501.

(23) Koga, T.; Barkley, D.; Nagao, M.; Taniguchi, T.; Carrillo, J.-M. Y.; Sumpter, B. G.; Masui, T.; Kishimoto, H.; Koga, M.; Rudick, J. G.;

Endoh, M. K. Interphase Structures and Dynamics near Nanofiller Surfaces in Polymer Solutions. *Macromolecules* **2018**, *51*, 9462−9470.
(24) Semenov, A. N.; Anastasiadis, S. H. Collective Dynamics of Polymer Brushes. *Macromolecules* **2000**, *33*, 613−623.
(25) Daoud, M.; Cotton, J. Star shaped polymers: a model for the conformation and its concentration dependence. *J. Phys. France* **1982**, *43*, 531−538.
(26) Förster, S.; Wenz, E.; Lindner, P. Density Profile of Spherical Polymer Brushes. *Phys. Rev. Lett.* **1996**, *77*, 95−98.
(27) Ohno, K.; Morinaga, T.; Takeno, S.; Tsujii, Y.; Fukuda, T. Suspensions of Silica Particles Grafted with Concentrated Polymer Brush: Effects of Graft Chain Length on Brush Layer Thickness and Colloidal Crystallization. *Macromolecules* **2007**, *40*, 9143−9150.
(28) Midya, J.; Rubinstein, M.; Kumar, S. K.; Nikoubashman, A. Structure of Polymer-Grafted Nanoparticle Melts. *ACS Nano* **2020**, *14*, 15505−15516.
(29) Wijmans, C. M.; Zhulina, E. B. Polymer Brushes at Curved Surfaces. *Macromolecules* **1993**, *26*, 7214−7224.
(30) Dukes, D.; Li, Y.; Lewis, S.; Benicewicz, B.; Schadler, L.; Kumar, S. K. Conformational Transitions of Spherical Polymer Brushes: Synthesis, Characterization, and Theory. *Macromolecules* **2010**, *43*, 1564−1570.
(31) Hore, M. J. A.; Ford, J.; Ohno, K.; Composto, R. J.; Hammouda, B. Direct Measurements of Polymer Brush Conformation Using Small-Angle Neutron Scattering (SANS) from Highly Grafted Iron Oxide Nanoparticles in Homopolymer Melts. *Macromolecules* **2013**, *46*, 9341−9348.
(32) Lo Verso, F.; Yelash, L.; Binder, K. Dynamics of Macromolecules Grafted in Spherical Brushes under Good Solvent Conditions. *Macromolecules* **2013**, *46*, 4716−4722.
(33) Klushin, L. I.; Skvortsov, A. M. Critical Dynamics of a Polymer Chain in a Grafted Monolayer. *Macromolecules* **1991**, *24*, 1549−1553.
(34) Lang, M.; Werner, M.; Dockhorn, R.; Kreer, T. Arm Retraction Dynamics in Dense Polymer Brushes. *Macromolecules* **2016**, *49*, 5190−5201.
(35) Reith, D.; Milchev, A.; Virnau, P.; Binder, K. Computer Simulation Studies of Chain Dynamics in Polymer Brushes. *Macromolecules* **2012**, *45*, 4381−4393.
(36) Mark, C.; Holderer, O.; Allgaier, J.; Hübner, E.; Pyckhout-Hintzen, W.; Zamponi, M.; Radulescu, A.; Feoktystov, A.; Monkenbusch, M.; Jalarvo, N.; Richter, D. Polymer Chain Conformation and Dynamical Confinement in a Model One-Component Nanocomposite. *Phys. Rev. Lett.* **2017**, *119*, 047801.
(37) Poling-Skutvik, R.; Olafson, K. N.; Narayanan, S.; Stingaciu, L.; Faraone, A.; Conrad, J. C.; Krishnamoorti, R. Confined Dynamics of Grafted Polymer Chains in Solutions of Linear Polymer. *Macromolecules* **2017**, *50*, 7372−7379.
(38) Wei, Y.; Xu, Y.; Faraone, A.; Hore, M. J. Local Structure and Relaxation Dynamics in the Brush of Polymer-Grafted Silica Nanoparticles. *ACS Macro Lett.* **2018**, *7*, 699−704.
(39) Wei, Y.; Chen, Q.; Zhao, H.; Duan, P.; Zhang, L.; Liu, J. Conformation and Dynamics along the Chain Contours of Polymer-Grafted Nanoparticles. *Langmuir* **2023**, *39*, 11003−11015.
(40) Miller, C. A.; Hore, M. J. A. Simulation of the Coronal Dynamics of Polymer-Grafted Nanoparticles. *ACS Polym. Au* **2022**, *2*, 157−168.
(41) Kotkar, S. B.; Howard, M. P.; Nikoubashman, A.; Conrad, J. C.; Poling-Skutvik, R.; Palmer, J. C. Confined Dynamics in Spherical Polymer Brushes. *ACS Macro Lett.* **2023**, *12*, 1503−1509.
(42) Chan, Y.-H. M.; Lenz, P.; Boxer, S. G. Kinetics of DNA-mediated Docking Reactions between Vesicles Tethered to Supported Lipid Bilayers. *Proc. Natl. Acad. Sci. U. S. A.* **2007**, *104*, 18913−18918.
(43) Bachmann, S. J.; Kotar, J.; Parolini, L.; Šarić, A.; Cicuta, P.; Di Michele, L.; Mognetti, B. M. Melting Transition in Lipid Vesicles Functionalised by Mobile DNA Linkers. *Soft Matter* **2016**, *12*, 7804−7817.
(44) McMullen, A.; Holmes-Cerfon, M.; Sciortino, F.; Grosberg, A. Y.; Brujic, J. Freely Jointed Polymers Made of Droplets. *Phys. Rev. Lett.* **2018**, *121*, 138002.
(45) Keane, D. P.; Mellor, M. D.; Poling-Skutvik, R. Responsive Telechelic Block Copolymers for Enhancing the Elasticity of Nanoemulsions. *ACS Appl. Nano Mater.* **2022**, *5*, 5934−5943.
(46) Keane, D. P.; Kolozsvary, T.; McDonald, B.; Poling-Skutvik, R. Bottlebrush Midblocks Promote Colloidal Bridging of Telechelic Polymers. *ACS Macro Lett.* **2024**, *13*, 1304−1310.
(47) Garg, N.; Carrasquillo-Molina, E.; Lee, T. R. Self-Assembled Monolayers Composed of Aromatic Thiols on Gold: Structural Characterization and Thermal Stability in Solution. *Langmuir* **2002**, *18*, 2717−2726.
(48) Yang, Y.; Yi, C.; Duan, X.; Wu, Q.; Zhang, Y.; Tao, J.; Dong, W.; Nie, Z. Block-Random Copolymer-Micellization-Mediated Formation of Polymeric Patches on Gold Nanoparticles. *J. Am. Chem. Soc.* **2021**, *143*, 5060−5070.
(49) Anderson, J. A.; Glaser, J.; Glotzer, S. C. HOOMD-blue: A Python package for high-performance molecular dynamics and hard particle Monte Carlo simulations. *Comput. Mater. Sci.* **2020**, *173*, 109363.
(50) Grest, G. S.; Kremer, K. Molecular dynamics simulation for polymers in the presence of a heat bath. *Phys. Rev. A* **1986**, *33*, 3628.
(51) Bishop, M.; Kalos, M. H.; Frisch, H. L. Molecular dynamics of polymeric systems. *J. Chem. Phys.* **1979**, *70*, 1299−1304.
(52) Poblete, S.; Wysocki, A.; Gompper, G.; Winkler, R. G. Hydrodynamics of discrete-particle models of spherical colloids: A multiparticle collision dynamics simulation study. *Phys. Rev. E* **2014**, *90*, 033314.
(53) Wani, Y. M.; Kovakas, P. G.; Nikoubashman, A.; Howard, M. P. Diffusion and sedimentation in colloidal suspensions using multi-particle collision dynamics with a discrete particle model. *J. Chem. Phys.* **2022**, *156*, 024901.
(54) Weeks, J. D.; Chandler, D.; Andersen, H. C. Role of repulsive forces in determining the equilibrium structure of simple liquids. *J. Chem. Phys.* **1971**, *54*, 5237−5247.
(55) Rubinstein, M.; Colby, R. H. Self-consistent theory of polydisperse entangled polymers: Linear viscoelasticity of binary blends. *J. Chem. Phys.* **1988**, *89*, 5291−5306.
(56) Likhtman, A. E.; McLeish, T. C. B. Quantitative Theory for Linear Dynamics of Linear Entangled Polymers. *Macromolecules* **2002**, *35*, 6332−6343.
(57) De Gennes, P. G. Reptation of a Polymer Chain in the Presence of Fixed Obstacles. *J. Chem. Phys.* **1971**, *55*, 572−579.

https://doi.org/10.1021/acsmacrolett.6c00205
ACS Macro Lett. XXXX, XXX, XXX−XXX